Image Segmentation Pipeline Based on Level Set and Topological Derivative

Danubia de Araujo Machado and André Antônio Novotny and Gilson Antonio Giraldi
National Laboratory for Scientific Computing
Petrópolis (RJ), Brasil
Web page: www.lncc.br

***Abstract*—In this work we propose a segmentation methodology based on the level set approach for boundary extraction and an optimization method formulated through the topological derivative. First, the methodology uses a low-pass filter and the topological derivative to get a rough definition of the boundaries of interest. Then, morphological operators are applied to fill holes and discard artifacts. Next, a level set model is used to improve the result giving the desired approximation. The obtained segmentation pipeline can be summarized by the following steps: (1) Pre-Processing: Low-Pass filtering; (2) Pre-Segmentation: Topological Derivative; (3) Post-Processing: Mathematical Morphology Operators; (4) Boundary extraction via level set method. The proposed methodology is applied for synthetic and biological (cell) image segmentation. The visual inspection shows that the obtained results are suitable and, in the case of synthetic images, the segmentation precision is quantified and outperforms another technique based only on the level set method.** [1]

***Keywords*-Image Segmentation; Topological Derivative; Boundary Extraction; Level Set Method**

I. Introduction

Image segmentation is a fundamental step for image analysis and computer vision tasks. Approaches in image segmentation can be roughly classified in [1]: (a) Contour Based methods, like active contours and active shape models; (b) Region based techniques; (c) Optimization approaches; (d) Clustering methods, like k-means, Fuzzy C-means, Hierarchical clustering; (e) Thresholding methods. In this paper we focus on contour based techniques, the level set approach [2], and an optimization method formulated through the topological derivative [3].

The level set method [4], [5], [6] has been successfully applied for boundary extraction, motion tracking and segmentation, mainly in medical imaging. In general, the process of boundary extraction in such applications involves some kind of pre-processing step [1]. Besides, the obtained result is sensitive to initialization conditions. On the other hand, segmentation techniques based on topological derivative needs (in general) a post-processing step, in order to improve the results [3].

Therefore, in this work we propose an image segmentation pipeline based on the topological derivative together with the level set method, which is the main improvement with respect to the previous work [3]. This pipeline combines the capabilities of the topological derivative to get a rough segmentation with the level set precision when initialized closer the target.

The topological derivative concept [7] quantifies the sensitivity of a given shape functional with respect to a singular domain perturbation, such as the nucleation of holes, inclusions, source-terms or even cracks. This concept, initially conceived to deal with topology optimization problems, has also been successfully applied to image segmentation [3]. Despite of the observed potential of the topological derivative, its result must be improved by a contour based approach, like level set. In this way, we are combining two segmentation methods: an optimization technique to get a first approximation of the boundary and the level set method to complete the segmentation. Besides, some low-pass filters and morphological operators can be also applied in order to improve the segmentation efficiency. The obtained segmentation pipeline is the main contribution of this work [8] and is composed by: (a) Low-pass Filtering; (b) Topological Derivative; (c) Mathematical Morphology; (d) Level Set Method. In addition we provide in [9] a full mathematical justification for the topological derivative formula [3].

Despite some theoretical study about connections between level set and the topological derivative [10], the combination of these techniques had not been explored in the image segmentation literature before our work. Another advantage of using level set in the last step is the possibility of exploring the topological capabilities of level set for multi-object segmentation and the fact that the methodology remains the same for 2D and 3D images. However, we can replace the level set by any other suitable deformable model.

The paper is organizes as follows. In sections II and III we describe the level set and the topological derivative techniques, respectively. Next, on section IV, the proposed methodology for segmentation is presented. The experimental results are discussed in section V. Finally, section VI offers final comment and further works.

II. Level Set

In this section we review some details of the level set formulation [2]. The main idea of this method is to represent the deformable surface (or curve) as a level set $\left\{x \in \Re^3 | G\left(x\right) = 0\right\}$ of an embedding function:

$$G : \Re^3 \times \Re^+ \rightarrow \Re, \tag{1}$$

[1] Full paper of M.Sc Dissertations.

such that the deformable surface (also called *front* in this formulation), at $t = 0$, is given by a surface S:

$$S\left(t=0\right) = \left\{x \in \Re^3 : G\left(x, t=0\right) = 0\right\}. \tag{2}$$

The next step is to find an Eulerian formulation for the front evolution. Following Sethian [2], let us suppose that the front evolves in the normal direction with velocity F that may be a function of the curvature, image gradient, etc.

We need an equation for the evolution of $G\left(x,t\right)$, considering that the surface S, at any time t, is the level set given by:

$$S\left(t\right) = \left\{x \in \Re^3 : G\left(x, t\right) = 0\right\}. \tag{3}$$

Let us take a point $x\left(t\right)$, $t \in \Re^+$ of the propagating front S. From its implicit definition given above we have:

$$G\left(x\left(t\right), t\right) = 0. \tag{4}$$

Now, we can use the Chain Rule to compute the time derivative of this expression:

$$G_t + F\left|\nabla G\right| = 0, \tag{5}$$

where $F = \left\|dx/dt\right\|$ is called the *speed function*. In this paper, the governing equation for the embedding function G , and, consequently, for the zero level set $S(t)$, has the general form [11]:

$$G_t = \left[\left(\frac{1+\lambda\kappa}{1+\left|\nabla I\right|^2}\right)\left|\nabla G\right| - \gamma(\nabla\left|\nabla I\right|\cdot\nabla G)\right], \tag{6}$$

where λ and γ are parameters that weight the different terms, κ is the curvature of the front, G is an embedding function, I is the image field and ∇ is the gradient operator. An initial condition $G\left(x, t=0\right)$ is required. A straightforward technique to define this function is to compute a signed-distance function as follows:

$$G\left(x, t=0\right) = \pm d, \tag{7}$$

where d is the distance from x to the surface $S\left(x, t=0\right)$ and the sign indicates if the point is interior (-) or exterior (+) to the initial front.

In this higher dimensional formulation, topological changes can be efficiently implemented. Stable Finite difference schemes, based on a uniform grid, can be used to solve equation (5). Besides, the update of the embedding function can be made cheaper if the narrow-band technique is applied [11]. Also, a stopping criterion is adopted as follows. We stop the evolution if: $N_m/N < e$, where N_m is the number of points that moved in one iteration, N is the total number of points of the front and e is a user-defined threshold.

III. Topological Derivative in Image Segmentation

Let us consider an open bounded domain $\Omega \subset \Re^2$, which is subject to a non-smooth perturbation confined in a small region $\omega_\varepsilon(\widehat{x}) = \widehat{x} + \varepsilon\omega$ of size ε, as shown in Figure 1. Here, $\widehat{x}$ is an arbitrary point of Ω and ω is a fixed domain of $\Re^2$.

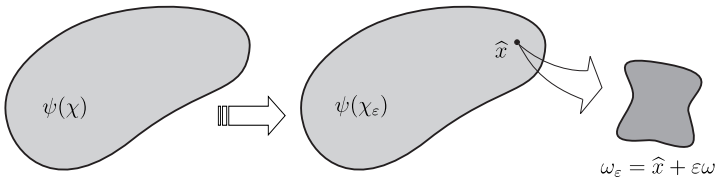

Fig. 1. The topological derivative concept.

Then, we assume that a given shape functional $\psi(\chi_\varepsilon(\widehat{x}))$, associated to the topologically perturbed domain, admits the following topological asymptotic expansion

$$\psi(\chi_\varepsilon(\widehat{x})) = \psi(\chi) + f(\varepsilon)D_\Omega(\widehat{x}) + o(f(\varepsilon)), \tag{8}$$

where $\psi(\chi)$ is the shape functional associated to the original (unperturbed) domain, $f(\varepsilon)$ is a positive function such that $f(\varepsilon) \to 0$, when $\varepsilon \to 0$. The function $\widehat{x} \mapsto D_\Omega(\widehat{x})$ is called the topological derivative of ψ at $\widehat{x}$. Therefore, this derivative can be seen as a first order correction of $\psi(\chi)$ to approximate $\psi(\chi_\varepsilon(\widehat{x}))$.

More precisely, the topological derivative $D_\Omega(\widehat{x})$ is a scalar function defined over the original domain that indicates, in each point, the sensitivity of the shape function when a singular perturbation of size ε is introduced at that point. In general, the domain singular perturbation can be, for instance: the introduction of holes, cracks or non smooth changes in the parameters of the problem (e.g., material properties, sources acting over the domain, boundary conditions, etc.).

Among the methods for calculation of the topological derivative currently available in the literature, here we shall adopt the methodology developed in [7], which is based on the following result:

$$D_\Omega\psi = \lim_{\varepsilon\to 0}\frac{1}{f'(\varepsilon)}\frac{d}{d\varepsilon}\psi(\chi_\varepsilon(\widehat{x})), \tag{9}$$

where $\frac{d}{d\varepsilon}\psi(\chi_\varepsilon(\widehat{x}))$ is the derivative of $\psi(\chi_\varepsilon(\widehat{x}))$ with respect to the small parameter ε, which can be seen as the sensitivity of $\psi(\chi_\varepsilon(\widehat{x}))$, in the classical sense, to the domain perturbation produced by a uniform expansion of the perturbation ω_ε [12], [13]. Therefore, we can use the concept of shape sensitivity analysis as an intermediate step in the topological derivative calculation [9].

A. Formulation of the Segmentation Problem

In [3] it was proposed a shape function that quantifies the misfit between the input image v being segmented and a possible segmentation u. Let us first define the input image v as

$$v \in \mathcal{V} = \{v \in L^2(\Omega) : v \text{ const. at image element (pixel) level}\}, \tag{10}$$

and the segmented image u as:

$$u \in \mathcal{U} = \{u \in \mathcal{V} : u(x) \in \mathcal{C}, \forall x \in \Omega\}, \quad (11)$$

where Ω is the image domain, and the set of classes $\mathcal{C}$ is given by:

$$\mathcal{C} = \{c_i \in \Re : i = 1, \cdots, N_c\}, \quad (12)$$

with N_c used to denote the number of classes in which the original image v will be segmented and c_i represents the intensity that characterizes the $i^{th}-class$. Therefore, let us introduce the following shape function, which is inspired on the Mumford-Shah functional [14]:

$$\psi(\chi) := \mathcal{J}(\varphi) = \frac{1}{2}\int_\Omega K\nabla\varphi\cdot\nabla\varphi + \frac{1}{2}\int_\Omega (\varphi - (v-u))^2, \quad (13)$$

where the field φ accounts for the misfit between v and u, and is the solution of the following variational problem: find $\varphi \in H^1(\Omega)$, such that:

$$\int_\Omega K\nabla\varphi\cdot\nabla\eta + \int_\Omega \varphi\eta = \beta\int_\Omega (v-u)\eta \quad \forall\eta \in H^1(\Omega). \quad (14)$$

The diffusive second order tensor field K is constant at image element level and $0 < \beta \leq 1$ is used to adjust the numerical algorithm. Note that the segmented image u and function φ can be seen as the control and the state, respectively. Therefore, the image segmentation problem can be stated as following: given the image data $v \in \mathcal{V}$, find the segmented image $u^* \in \mathcal{U}$ such that minimizes the functional (13).

In this process, the topological derivative is used to design an algorithm that follows a steepest descent methodology (see section IV). It can be shown that, for the functional 13, the topological derivative $D_\Omega(\widehat{x})$ is given by:

$$D_\Omega(\widehat{x}) = -\frac{1}{2}|\omega|(u-c_i)[(\varphi(\widehat{x}) - (v-u))] -$$

$$\frac{1}{2}|\omega|(u-c_i)[(\varphi(\widehat{x}) - (v-c_i)) + 2(1-\beta)\varphi(\widehat{x})], \quad (15)$$

where function $f(\varepsilon) = \varepsilon^2$ and $|\omega|$ stands by the Lebesgue measure of the set ω ($\omega = \pi$ in $\Re^2$).

IV. Proposed Method

The proposed segmentation methodology is composed by the following pipeline: (1) Pre-Processing: Low-Pass filtering; (2) Pre-Segmentation: Topological Derivative; (3) Post-Processing: Mathematical Morphology Operators; (4) Boundary extraction via level set method.

Medical and biological images have a complex intensity field and texture patterns. Thus, the low-pass filtering (a) is applied to smooth the original image before using the topological derivative. This improves the robustness of the pipeline against parameters choice. The morphological operators (c) are used to simplify the level set initialization.

As mentioned before, for the image $v \in \mathcal{V}$ we need to find the segmented image $u^* \in \mathcal{U}$ that minimizes the shape function $\mathcal{J}(\varphi)$ by successively selecting the class that produces a negative value of the topological derivative. In this way, the following image segmentation algorithm is proposed (Algorithm 1) based on the topological derivative.

Algorithm 1 Image segmentation based on the topological derivative

Require: An input image $v \in \mathcal{V}$, the set $\mathcal{C}$, an initial guess $u \in \mathcal{U}$, the diffusivity tensor field K and the parameters β and the step size $\alpha \in (0, 1)$.
Ensure: The segmented image $u^* \in \mathcal{U}$.
  while $D_\Omega(\widehat{x}) < 0$ **do**
    find the solution φ to the variational problem (14)
    evaluate $D_\Omega(\widehat{x}) = D_\Omega(\widehat{x}, c_i)$ according to (15)
    compute $c^*(\widehat{x}) = \arg\min_{c_i \in \mathcal{C}}\{D_\Omega(\widehat{x}, c_i)\}$
    compute $d_T^* = \min_{\widehat{x}\in\Omega}\{D_\Omega(\widehat{x}, c^*(\widehat{x}))\}$
    if $D_\Omega(\widehat{x}, c^*(\widehat{x})) \leq (\alpha)d_T^*$, set $u(\widehat{x}) = c^*(\widehat{x})$
    update the class $\mathcal{C}$ according to Algorithm 2
  end while
  $u = u^*$

The solution φ in Algorithm 1 is obtained by the standard finite element method, where the bilinear elements coincide with the image pixels.

Obviously, a fundamental question is: How to define the set of classes $\mathcal{C}$? This is performed by calling the Algorithm 2, after each interaction of the main loop. Basically, the Algorithm 2 takes an initial guess $\mathcal{C}$ (minimum and maximum intensity values for two-class case) and computes $\mathcal{C}^\delta$, for $\delta \in \{-1, 0, 1\}$, and replaces the class $\mathcal{C}$ by the $\mathcal{C}^\delta$ that minimizes the functional $\mathcal{J}(\varphi)$ in expression (13).

The topological derivative result may have holes inside the objects of interest as well as artifacts in the background. These problems can be easily removed through simple morphological operators (erosion, dilation, region filling). The obtained result is binarized (0 for the background and 1 inside the objects).

Algorithm 2 Adjust the values of the classes

Require: An input image $v \in \mathcal{V}$, the set $\mathcal{C}$ and the segmented image $u \in \mathcal{U}$ obtained at each iteration of Algorithm 1.
Ensure: The new set of classes $\mathcal{C}^*$.
  $\mathcal{C}^* = [\,]$
  for $c_i \in \mathcal{C}$ **do**
    for $\delta = -1$ to 1 **do**
      set $\mathcal{C}^\delta = (\mathcal{C} \setminus \{c_i\}) \cup \{c_i + \delta\})$
      compute $\psi^\delta = \mathcal{J}(\varphi)$ by taking $u \in \mathcal{C}^\delta$
    end for
    set $c^* = c_i + \delta^*$, where $\delta^* = \min_{\delta\in\{-1,0,1\}}\{\psi\delta\}$
    set $\mathcal{C}^* = \mathcal{C}^* \cup \{c^*\}$
  end for
  $\mathcal{C} = \mathcal{C}^*$

Then, this result is the input for the computation of the signed-distance function of expression (7) to initialize the level set method, described in section II. For to get as the zero level set is used a simple $2D$ marching cubes. In this way, we get

a first approximation of the boundary which can save time computation and improve the accuracy of the level set result.

V. Experimental Results

In this section we show the robustness and efficiency of the proposed segmentation approach. We start by considering a synthetic image of size 228×184 pixels with three classes $\{c_1, c_2, c_3\}$ as shown in Figure 2.(a). This image is composed by two concentric circles; the inner one with 31 pixels of radius ($c_1 = 50$); the outer one with 71 pixels of radius ($c_2 = 100$); and a background with image intensity $c_3 = 204$. Then this image is damaged with a gaussian noise of null mean and variance 0.05, as can be seen in Figure 2.(b). The idea is to segment the damaged image into three classes using the proposed method (section IV) and then compare the result with level set (section II) alone.

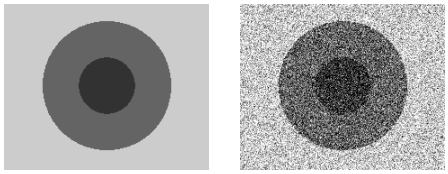

(a) (b)

Fig. 2. (a) Synthetic image. (b) Damaged image with 5% of white noise.

Before starting, we must choose a low-pass filter. Three filters have been tested: (1)Directional, due to its capability to preserve edges; (2) Mean and gaussian which are known low-pass techniques very much used in image processing.

Figure 2.(b) was filtered 8 times by each filter and the result was segmented using the proposed pipeline. The initial guess for the set C is the $minimum$, $(minimum + maximum)/2$ and $maximum$ intensities of the original image at startup. The setting of parameters was performed through experimentation following the references [3], [11]. The pre-segmentation results, obtained through the Algorithm 1 applied to the filtered versions of image 2.(b), are shown in Figure 3 using the following parameter values: $\beta = 0.3$, $\alpha = 1.0$ e $k = 20$.

A visual inspection of Figures 3.(a)-(c) shows that the mean filter gives the best pre-segmentation result. So, we take the image field of Figure 3.(c) for the level set initialization in the last step of the pipeline. For the sake of simplicity, each image feature is segmented separately. The Table I shows the precision of the segmentation result (First line: "Mean-PM" means the mean filtered image segmented with the proposed method). The precision of the obtained segmentation is analyzed through the following error measure:

$$Error = \sum_{i=1}^{N} \frac{|r - d_i|}{N} \tag{16}$$

where r is the radius of the circle of interest in Figure 2.(a) and d_i, com $i = 1, 2, ..., N$, represent the distances from the points of zero level set to the center of that circle.

In order to compare our approach with the level set method alone, the filtered images are segmented by using level set

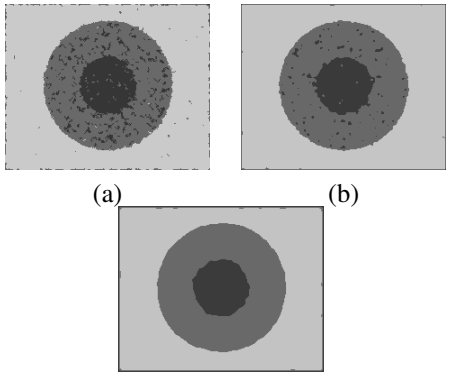

(a) (b)

(c)

Fig. 3. Topological derivative results: (a)Directional filtered image: after 53 iterations of Algorithm 1. (b) Gaussian filtered image: after 52 iterations of Algorithm 1. (c) Mean filtered image: after 45 iterations of Algorithm 1.

initialized by hand, as shown in Figures 4.(a)-(d) for the mean filtered image only. Once again, for the sake of simplicity, each image feature is segmented separately. According to [11], we have used a time step $\Delta t = 0.005$, stop criterion $e = 10^{-5}$ and parameters $\lambda = 50$ and $\gamma = 10$. The Table I shows the error, computed by expression (16) for each result (Last line: "Mean-LS" means the mean filtered image segmented with the level set method, and so on).

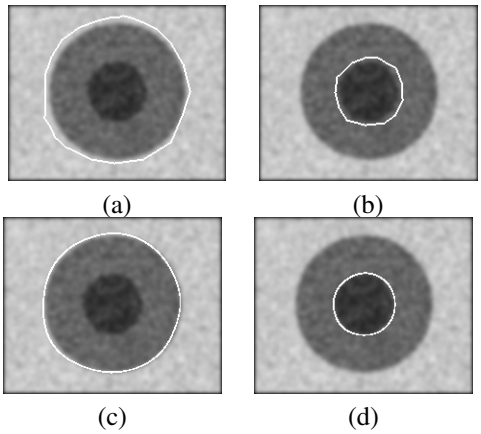

(a) (b)

(c) (d)

Fig. 4. Level Set method for mean filtered image: (a) Outer circle initialization. (b) Inner circle initialization. (c) Final result for outer circle after 505 iterations. (d) Segmentation result for inner circle after 257 iterations.

Despite of the fact that the level set initialization (given by the user) was too close to the boundaries of interest, the Table I shows that the proposed pipeline outperforms the level set results. Also, we should emphasize that our method does not depend on user interaction. In fact, as already known in deformable models, depending on the chosen initialization the segmentation may be not precise. Besides, the first and last line of this table indicate that the mean filter is the best one for the pre-processing step.

TABLE I
PRECISION OF THE PROPOSED METHODOLOGY (PM) AND THE LEVEL SET TECHNIQUE (LS).

Error Computed by Expression (16)		
	Outer Circle	Inner Circle
Mean-PM	0.4929	0.6821
Directional-LS	3.3061	1.5912
Gaussian-LS	2.4561	2.1548
Mean-LS	1.7356	1.2375

Now, we use the proposed pipeline presented in section IV for cell segmentation. Therefore, it is assumed that we may have more than one object of interest in the image. However, we are supposing that each object boundary have the properties of connectedness and closedness. Therefore, we can fill inner holes and we can discard foreground regions linked with the image boundary.

The test images were obtained by electron microscopy techniques [15], [16]. Our goal in these experiments is to verify the computational time as well as the robustness of the parameters for a specific application, which is a desired feature for the methodology.

We apply the mean filter for the pre-processing step because it generates better results for synthetic images. In this case we assume two classes. Therefore, the set C is initialized with the $minimum$ and $maximum$ intensities of the original image.

As an example, let us observe the Figure 5.(a), pig cells, whose resolution is 197 (width) x 102 (height) pixels. This image has some noise and artifacts in the background. Figure 5.(b) draws the topological derivative result. In this case, we have more than one object of interest which were pre-segmented by the Algorithm 1. However, this result must be improved by discarding cell regions linked with the image boundary as well as artifacts in the background. The former is discarded by a simple automatic inspection. To discard the later, we need a set of pre-defined features (area, for example), and corresponding lower bounds. For small artifacts we can also use morphological operators (opening or closing). In the case of Figure 5.(b) an area lower bound is more efficient because morphological operators may corrupt the regions of interest. It is important to stress that post-processing scheme is application dependent but it can be customized if we know the scale (size) range of the objects of interest. For instance, in the case of Figure 5.(b), as well as some of the test image set, the area lower bound was $P = 180$ (see [17], Chapter 5).

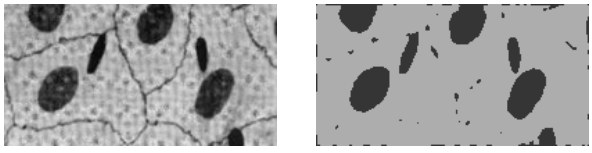

(a) (b)

Fig. 5. (a) Pig tissue cells. (b) Topological derivative result after 49 iterations of Algorithm 1.

The result obtained after the post-processing is used for the level set initialization, pictured on Figure 6.(a). The desired result, shown in Figure 6.(b), is obtained after 4 interactions of the level set. The values of the parameters used are: for the topological derivative we set $\beta = 0.3$, $\alpha = 1.0$, $k = 20$ and for level set we use $\Delta t = 0.004$, $e = 10^{-2}$, $\lambda = 15$ e $\gamma = 10$. Once the level set starts very close the target it is difficult to see differences between the boundaries in Figures 6.(a)-(b). In the following examples we will return to this point.

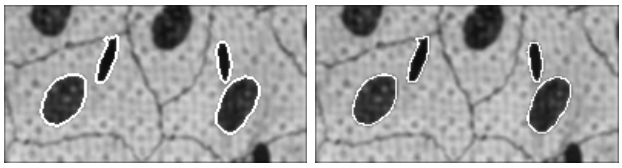

(a) (b)

Fig. 6. (a) Level set initialization. (b) Final segmentation after 4 iterations of the level set method.

The next example, pictured on Figure 7.(a), shows the cell image of a canguru with resolution of 249 (width) x 195 (high) pixels. We can observe the presence of texture patterns in the background. Figure 7.(b) shows the result of the topological derivative. We observe holes inside the region of interest as well as artifacts in the background due to inhomogeneities in the intensity pattern. So, we apply a region filling algorithm in order to fill holes inside the object. Then, the opening operator is used, with the square structuring element of size $W = 6$, in order to discard background artifacts.

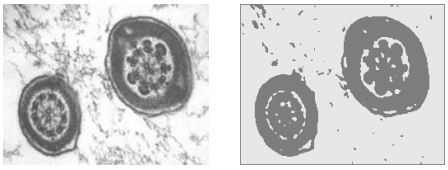

(a) (b)

Fig. 7. (a) Canguru cell with resolution 249 (width) $\times$ 195 (height) pixels. (b) Topological derivative result after 57 iterations (Algorithm 1)

The result allows to get a suitable initialization for the level set method, as we can see in Figure 8.(a). After 9 interactions we obtain the desired result, shown in Figure 8.(b). The choice of parameters is the same as the previous result.

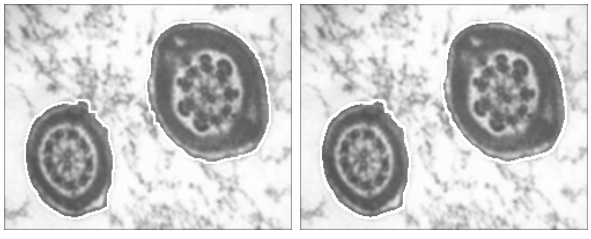

(a) (b)

Fig. 8. (a) Initialization of the level set technique. (b) Target boundary after 9 iterations of the level set technique.)

A visual inspection shows little changes between the level

set result and its initialization for the above examples. However, if we add noise things become very different. Figure 9.(a) shows an image that was corrupted with a gaussian noise of mean null and variance 0.8 and the level set initialization obtained with our proposed methodology (see [9] for details).

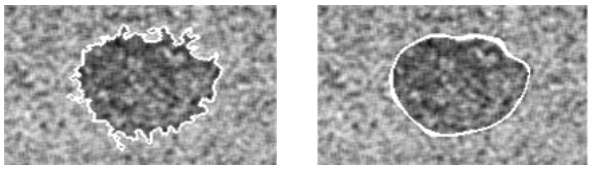

(a) (b)

Fig. 9. (a) Level set initialization in the last step of the proposed method. (b) Level set result after 135 interactions.

In this case, the initialization of the level set is not so close to the desired boundary as we observed in the above examples. Despite of this, a visual inspections shows that we get the desired result after 135 interactions. The values of the parameters used are: $\beta = 0.2$, $e = 10^{-5}$, $\lambda = 30$ and $\Delta t = 0.005$. The others are the same of the example of Figure 6.

The cells pictured in Figures 5-8 belong to an image database composed by 12 images (see [17], Chapter 5). We apply the proposed pipeline to this images keeping the mean filter for pre-processing. The post-processing stage was implemented using area lower bounds, fill roles and opening operator. The parameters values for the level set method remained unchanged for all tests. The topological derivative parameters do not undergo modifications for 9 images. Even the synthetic experiment keeps these values. For the others three cell images we need to redefine just the β parameter: 0.5, 0.6 and 0.7. These results show a suitable robustness of the parameters which is a desired feature for the model.

The computational cost of the proposed pipeline is basically determined by the level set and the topological derivative because the other methods are too fast. We have used a PC with Intel Core 2 CPU, 2.80GHz, and RAM memory of 2.5GB, running a single core Matlab implementation.

We did not implement narrow band techniques for level set. So, its computational cost depends on the image resolution and the number of iterations. The same happens for the topological derivative. The range of image resolutions used was between $[144 - 249]$ for width the and $[102 - 244]$ for the height. The maximum number of iterations for the level set was 9 and the maximum CPU time was 0.1235 seconds for this method. For the topological derivative, the range $[min, max]$ for the number of iterations was $[49, 254]$ with CPU time range $[53.6284, 708.9881]$, in seconds (see [17], Chapter 5, for details). We note that it represents the main contribution to the computational cost of the proposed approach. A new optimized implementation must be provided soon.

VI. Conclusion and Future Works

In this work we propose an image segmentation approach based on topological derivative and level set methods. We have shown results for a synthetic image using the level set method and the proposed pipeline. Finally, the last approach was applied in the case of real image segmentation. We have obtained an image segmentation with acceptable quality using the proposed pipeline, even in the presence of noise. In particular, the boundaries of the image features are smoother than the ones obtained by single topological derivative. In addition, the topological derivative gives a quite good initial guess for the level set method, improving the final result and allowing to automatically deal with multi-object segmentation. Further research directions are to optimize the topological derivative implementation and to test the approach for $3D$ image data sets. Besides, we should provide a comparative evaluation of the proposed method with other segmentation techniques as well as more robust level set implementations [1] for both segmentation precision and performance.

References

[1] J. Suri, D. Wilson, and S. Laxminarayan, *Handbook of Biomedical Image Analysis: Volumes I, II: Segmentation Models*. Kluwer Academic/Plenum Publishers, 2005.

[2] R. Malladi, J. A. Sethian, and B. C. Vemuri, "Shape modeling with front propagation: A level set approach," *IEEE Trans. Pattern Anal. Mach. Intell.*, vol. 17, no. 2, pp. 158–175, 1995.

[3] I. Larrabide, R. A. Feijóo, A. A. Novotny, and E. A. Taroco, "Topological derivative: A tool for image processing," *Comput. Struct.*, vol. 86, no. 13-14, pp. 1386–1403, 2008.

[4] S. Yan, J. Yuan, and C. Hou., "Segmentation of medical ultrasound images based on level set method with edge representing mask," in *Advanced Computer Theory and Engineering, 3rd International Conference*, vol. 2, 2010, pp. V2–85–V2–88.

[5] M. Strumia, D. Feltell, N. Evangelou, P. Gowland, C. Tench, and L. Bai., "Grey matter segmentation of 7T MR images," in *IEEE Nuclear Science Symposium and Medical Imaging Conference*, 2011, pp. 3710–3714.

[6] L. H. Chieh., "Shape-Based Level Set Method for Image Segmentation," in *Proc. Int. Conf. Hybrid Intelligent Systems*, 2009, pp. 243–246.

[7] A. A. Novotny, R. A. Feijóo, E. Taroco, and C. Padra, "Topological sensitivity analysis," *Computer Methods in Applied Mechanics and Engineering*, vol. 192, no. 7-8, pp. 803–829, 2003.

[8] D. Machado, G. Giraldi, and A. Novotny, "Segmentation approach based on topological derivative and level set." in *17th International Conference on Systems, Signals and Image Processing, Rio de Janeiro*, 2010, pp. 85–88.

[9] ——, "Multi-object segmentation approach based on topological derivative and level set method," *Integrated Computer-Aided Engineering*, vol. 18, no. 4, pp. 301–311, 2011.

[10] L. He and S. Osher, "Solving the chan-vese model by a multiphase level set algorithm based on the topological derivative," in *SSVM'07: Proc. of the 1st Int. Conf. on Scale Space and Variational Methods in Comp. Vis.*, 2007, pp. 777–788.

[11] J. S. Suri, K. Liu, S. Singh, S. Laxminarayan, X. Zeng, and L. Reden, "Shape recovery algorithms using level sets in 2-d/3-d medical imagery: a state-of-the-art review." *IEEE Transactions on Information Technology in Biomedicine*, vol. 6, no. 1, pp. 8–28, 2002.

[12] M. Delfour and J. Zolésio, *Shapes and Geometries. Advances in Design and Control*. Philadelphia: SIAM, 2001.

[13] J. Sokołowski and J. Zolésio, *Introduction to shape optimization - shape sensitivity analysis*. New York: Springer-Verlag, 1992.

[14] D. Mumford and J. Shah, "Optimal approximations by piecewise smooth functions and associated variational problems," *Comm. Pure Appl. Math.*, vol. 42, no. 5, pp. 577–685, 1989.

[15] C. Mims, "Ubc biomedia image and movie database." [Online]. Available: www.biomedia.cellbiology.ubc.ca

[16] T. U. of Queensland Austrália, "Centre for microscopy and microanalysis," 2007. [Online]. Available: http://www.uq.edu.au/nanoworld/

[17] D. Machado, "Segmentação de imagens via método dos conjuntos de níveis e derivada topológica," 2012. [Online]. Available: virtual01.lncc.br/~giraldi/DissertacaoMachado.pdf